

Thermal decomposition on Aceox[®] BTBPC mixed with hydrochloric acid

Sheng-Yi Lin¹ · Chi-Min Shu² · Yun-Ting Tsai¹ · Wei-Chun Chen¹ · Kuang-Hua Hsueh³

Received: 20 November 2014 / Accepted: 23 June 2015 / Published online: 21 July 2015
© Akadémiai Kiadó, Budapest, Hungary 2015

Abstract 1,1-Bis(*tert*-butylperoxy)cyclohexane (BTBPC) has two active O–O peroxide groups and is usually used as an initiator in a chemical process. However, it also easily accelerates decomposition in the presence of certain catalysts. This paper discusses the runaway reactions of BTBPC alone or mixed with various concentrations of hydrochloric acid (HCl, 1.0, 2.0, 4.0, and 8.0 N). Essential thermokinetic parameters, including apparent exothermic onset temperature (T_o), peak temperature (T_p), apparent activation energy (E_a), heat of decomposition (ΔH_d), and rate constant (k), were evaluated by differential scanning calorimetry under the heating rates of 1.0, 2.0, 4.0, and 8.0 °C min⁻¹. A kinetics-based curve fitting method was employed to appraise the possible kinetic models and their thermokinetic parameters at 4.0 °C min⁻¹ heating rate. All the BTBPC HCl mixtures have two exothermic peaks, but BTBPC alone and BTBPC mixed with 1.0 N HCl have just only one. 4.0 N HCl mixture has two endothermic peaks. T_o of the first peak in 8.0 N HCl mixtures is shifted to lower temperatures, 46.1 °C. The model of BTBPC is a single-stage

reaction; however, BTBPC mixed with 1.0 or 2.0 N HCl is a two-stage decomposition reaction. Moreover, 4.0 or 8.0 N HCl mixture is three- and five-stage decomposition reaction, respectively. As more concentrated HCl is being mixed, kinetic models become more complex.

Keywords 1,1-Bis(*tert*-butylperoxy)cyclohexane (BTBPC) · Curve fitting method · DSC · Hydrochloric acid (HCl) · Kinetic models

List of symbols

$2E_a$	Apparent activation energy of reaction (kJ mol ⁻¹)
ΔH_{\max}	Maximum heat release (kJ kg ⁻¹ min ⁻¹ , or W g ⁻¹)
ΔH_d	Heat of decomposition (kJ kg ⁻¹)
ΔH_p	Heat release of peak (kJ kg ⁻¹)
ΔH_t	Total heat release (kJ kg ⁻¹)
k	Reaction rate constant (s ⁻¹)
k_o	Pre-exponential factor in the Arrhenius equation (s ⁻¹ M ¹⁻ⁿ)
m	Mass of reactant (g)
N	Normality of hydrochloric acid (HCl) (eq mol ⁻¹)
n	Order of reaction (dimensionless)
n_i	Reaction order of <i>i</i> th stage (dimensionless)
R	Ideal gas constant (8.314 J mol ⁻¹ K ⁻¹)
r	Reaction rate (g s ⁻¹)
r_{rcrn}	Reaction rate for the reactant in each stage of reaction (g s ⁻¹)
T_o	Apparent exothermic onset temperature of decomposition reaction (°C)
T_p	Peak temperature of thermal curve by DSC detector (°C)
z	Autocatalytic constant (variable)
α	Degree of conversion of reaction (dimensionless)

✉ Kuang-Hua Hsueh
suhua@mail.hwai.edu.tw

¹ Graduate School of Engineering Science and Technology, National Yunlin University of Science and Technology (YunTech), 123, University Rd., Sec. 3, Douliou, Yunlin 64002, Taiwan, ROC
² Department of Safety, Health, and Environmental Engineering, YunTech, 123, University Rd., Sec. 3, Douliou, Yunlin 64002, Taiwan, ROC
³ Department of Safety, Health, and Environmental Engineering, Chung Hwa University of Medical Technology, 89, Wen-Hwa 1st St., Jen-te, T'ai-nan 71703, Taiwan, ROC

α_{rcm}	Degree of conversion for the reactant in each stage of reaction (dimensionless)
β	Heating rates of DSC experiment ($^{\circ}\text{C min}^{-1}$)

Introduction

A relatively weak oxygen–oxygen linkage (bond dissociation energy of 29.0–47.0 kcal mol⁻¹) is characteristic of organic peroxide molecules (OPs) [1]. The unusual weakness of the bivalent –O–O– bond is probably due to the electronic structure of peroxides and the relatively high electronegative character of the oxygen atoms. Within a structural series of the peroxy compounds, sensitivity and instability increase as active oxygen content and oxygen balance increase [2]. Heat, mechanical shock, friction, shaking, or contaminations can initiate explosive decomposition of many organic peroxides. It is also easy to accelerate decomposition in the presence of certain mineral acid catalysts [3, 4].

OPs are dangerous materials widely used in the chemical and process industry. They are often used as an initiator to induce free radicals in the initiation of polymerization reaction, especially in the manufacturing of plastics and rubbers [5]. Numerous incidents involving OPs have been reported often owing to a runaway reaction [6, 7]. Over the past four decades, many studies have focused mostly on the incompatible reaction of monoperoxy functional OPs with organic solvents, metal ions, and acid contaminants [8, 9, 19–21]. Little attention has been devoted to the thermal hazards of diperoxy functional OPs.

Aceox[®] BTBPC is a commercial chemical product widely used in the plastic and rubber industries. Its main ingredient, 1,1-bis(*tert*-butylperoxy)cyclohexane (BTBPC), is shown in Fig. 1 [10]. BTBPC is used as a symmetrical difunctional peroxide initiators of bulk styrene polymerization [11]. This symmetrical peroxyketal peroxide can yield a higher rate of polymerization and a lower residual styrene content. Aceox[®] BTBPC can initiate polymer growth from two different sites within the same fragment, and then higher molecular weight polystyrene (PS) can be generated at faster rates than

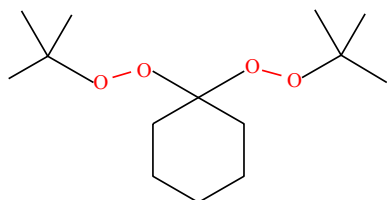


Fig. 1 Structure of 1,1-bis(*tert*-butylperoxy)cyclohexane [10]

applying monofunctional initiators [12]. Although BTBPC is one of the most commonly used initiators for the PS and its copolymers, its thermokinetic characteristics and thermal runaway reaction by mixing with mineral acid contaminants have not been well elucidated yet.

Owing to the hazardous consequences of decomposition of BTBPC and its extensive use in the polymer industry, we conducted this study to establish the runaway reaction phenomena of BTBPC mixed with hydrochloric acid (HCl) as a typical contaminant. We researched the basic thermokinetic characteristics and thermal runaway reaction of BTBPC alone and mixed with fixed mass of hydrochloric acid contaminants by thermokinetic evaluation. We applied the experimental data obtained from the differential scanning calorimetry (DSC) at heating rates of 1.0, 2.0, 4.0, and 8.0 $^{\circ}\text{C min}^{-1}$, by using curve fitting to evaluate the kinetic parameters and inherent safety characteristics of its thermal decomposition, including reaction order (n), apparent exothermic onset temperature (T_o), apparent activation energy (E_a), heat of decomposition (ΔH_d), and rate constant (k). Based on the stability of reaction and length of this paper, estimating kinetic models to acquire more detailed reaction mechanisms and possible decomposition pathways at 4.0 $^{\circ}\text{C min}^{-1}$ heating rate is our concern.

Experimental

Samples

Aceox[®] BTBPC is a light yellowish liquid, peroxyketal peroxide, and 70.0 mass% purity in isoparaffin hydrocarbon solvent. Its main ingredient, BTBPC, has a pair of symmetrical oxygen–oxygen peroxide groups as illustrated in Fig. 1. We purchased it directly from ACE Chemical Corp. and stored in a refrigerator at 4.0 $^{\circ}\text{C}$ to keep it stable and away from any external hot conditions. Four types of solutions were used as contaminants for testing the mixing conditions, including 1.0, 2.0, 4.0, and 8.0 normality (N) of hydrochloric acid (HCl). We selected compounds of HCl to compare the effects of different concentrations of acidity on BTBPC. The pure HCl, obtained from Fluka Corp., was diluted with deionized water to acquire the above-mentioned various concentrations of HCl and then stored in a refrigerator at 4.0 $^{\circ}\text{C}$. The quantitative specific contaminants (1.2–2.3 mg) were added into gold-plated high-pressure crucibles and mixed with BTBPC 70.0 mass% (1.7–3.9 mg).

Differential scanning calorimetry (DSC)

DSC can be employed to detect the temperature difference between the sample and reference. From these references,

the heat flow can be detected immediately for viewing on the thermal curves. Dynamic temperature-programmed screening experiments were conducted on a Mettler TA 8000 system and coupled with a DSC 821^c, gold-plated high-pressure measuring test crucible (Mettler ME-00026732) [13]. Crucibles serve as containers for samples during thermoanalytical measurements and cannot be reused. The maximum withstand pressure is ca. 15.0 MPa. A lid is pressed onto the crucible with a pressure of about a ton so that the seal tightens the crucible, and a toggle press is applied to close the crucible. The built-in STAR^c software was applied to acquire thermal curves [14]. At the beginning of an experiment, DSC had to be stabilized for 30.0 min, and then the experiments were started with a specific heating rate for better thermal equilibrium. The scanning heating rates of this study were selected as 1.0, 2.0, 4.0, and 8.0 °C min⁻¹ for each condition of experiments [15]. The range of temperature rise was from 30.0 to 300.0 °C for each experiment. After the DSC test, the crucible was weighed again to confirm that there was no leakage during the experiment.

This apparatus could properly acquire the heat flow, and then, via experimental data we could calculate T_o , the maximum temperature at which the peak point (T_p) occurred, and heat of decomposition (ΔH_d) by the interior built-in STAR^c software of DSC. We used curve fitting to acquire the thermokinetic parameters based on the experimental data of time (s), temperature (°C), and heat power (mW). These data and thermokinetic evaluation were implemented by applying thermal safety software (TSS) developed by CISP Ltd. [16]. The methods are clearly and completely described by Kossoy and Akhmetshin [17] for the creation of a thermokinetics model and the algorithms that are adopted. After these experimental data were fitted, thermokinetic parameters could therefore be obtained.

Results and discussion

Preliminary observations of original thermal waveforms

All the mass constituents of the hazardous material (BTBPC) and its HCl contaminant mixtures are listed in Table 1. The mass ratio (w/w) of BTBPC to HCl was kept about 1.75 ± 0.55 to ensure the consistency of results of concentration gradient of HCl affected in BTBPC. Figure 2 shows the untreated original thermal waveforms of BTBPC at heating rates of 1.0, 2.0, 4.0, and 8.0 °C min⁻¹, respectively. It demonstrates that they are a single smooth curve (peak A); Table 2 shows T_o as well as T_p and ΔH_{max} of exothermic peak A increased with increase in heating rates. Figure 3 shows the untreated original thermal waveforms of BTBPC

alone and mixed with 1.0, 2.0, 4.0, and 8.0 N HCl at heating rates of 1.0, 2.0, 4.0, and 8.0 °C min⁻¹, respectively. If BTBPC was mixed with 1.0 N HCl, just like BTBPC alone, there would be no significant change in the thermal waveform, T_o , T_p , and ΔH_{max} of exothermic peak A (Fig. 3a). However, as shown in Fig. 3b, differences appeared in the thermal waveforms of 2.0 N HCl mixture under the heating rates of 1.0, 2.0, and 8.0 °C min⁻¹. There are two small peaks split on both sides of exothermic peak A: one is peak A-1 (103.0, 112.6, 125.5 °C) and the other is peak A-2 (169.3, 172.9, 192.0 °C). Surprisingly, under the heating rate of 4.0 °C min⁻¹, peak A did not split into two small peaks (as mentioned above, peaks A-1 and A-2) and still kept the same waveforms just like BTBPC alone or 1.0 N HCl mixture.

When BTBPC was mixed with more highly concentrated HCl, such as 4.0 or 8.0 N under the heating rates of 1.0, 2.0, 4.0, and 8.0 °C min⁻¹, as shown in Fig. 3c, d, the exothermic peak A vanished, with exothermic peak A-1 and exothermic peak A-2 remaining. Figure 3c shows T_p and ΔH_{max} of peak A-1 and peak A-2 are 85.9–108.1 °C, 1.0–6.0 W g⁻¹, and 150.3–177.4 °C, 0.1–0.3 W g⁻¹ in BTBPC mixed with 4 N HCl under the heating rates of 1.0, 2.0, 4.0, and 8.0 °C min⁻¹, respectively. If BTBPC was mixed with 8 N HCl under the heating rates of 1.0, 2.0, 4.0, and 8.0 °C min⁻¹, as shown in Fig. 3d, T_p and ΔH_{max} of peak A-1 and peak A-2 are 67.6–89.9 °C, 0.9–2.2 W g⁻¹, and 130.1–184.0 °C, 0.3–0.7 W g⁻¹, respectively. All increased with increase in heating rates.

As a brief summary, the exothermic peaks of waveforms in BTBPC alone and BTBPC mixed with 1 N HCl at heating rates of 1.0, 2.0, 4.0, and 8.0 °C min⁻¹ are all a single smooth curve. The exothermic peak of waveform in BTBPC mixed with 2.0 N HCl at heating rate of 4.0 °C min⁻¹ is still a single smooth curve. However, it splits into three exothermic peaks at heating rates of 1.0, 2.0, and 8.0 °C min⁻¹. The exothermic peak of waveforms in BTBPC mixed with 4.0 or 8.0 N HCl at heating rates of 1.0, 2.0, 4.0, and 8.0 °C min⁻¹ splits into two exothermic peaks. With increasing concentration of HCl, T_o shifted to higher temperatures; however, T_p shifted to lower temperatures. Moreover, with increasing heating rates, T_p shifted to higher temperatures and ΔH_{max} increased.

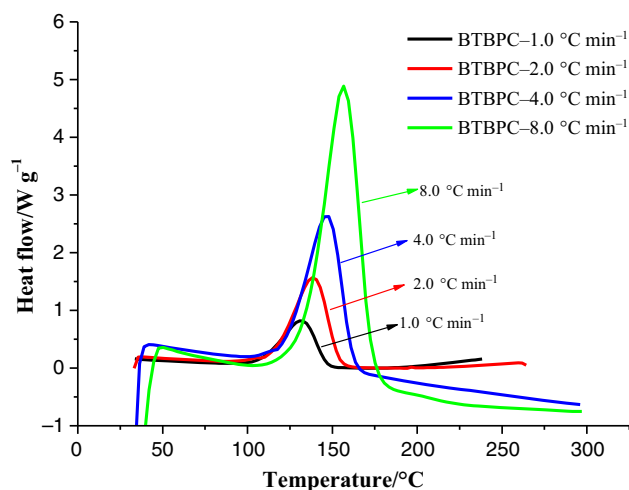
Thermal hazard analysis of thermal waveforms

To clearly compare BTBPC and its contaminant mixtures of 1.0, 2.0, 4.0, or 8.0 N HCl, Figs. 4–6 show the thermal waveforms at the single heating rate of 4.0 °C min⁻¹, respectively. Relevant thermokinetic parameters are presented in Table 3. It summarizes the thermokinetic parameters derived from the DSC data sets by the device's built-in STAR^c software, including the exothermic apparent onset temperature (T_o), peak temperature (T_p), maximum heat

Table 1 Constituents of BTBPC and its HCl contaminant mixtures

Sample item	$\beta/^\circ\text{C min}^{-1}$	Constituents			BTBPC/HCl/mg/mg
		BTBPC/mg	HCl/mg	Total mass/mg	
BTBPC	1.0	4.6	–	4.6	–
	2.0	5.2	–	5.2	–
	4.0	2.6	–	2.6	–
	8.0	4.6	–	4.6	–
BTBPC + HCl (1.0 N)	1.0	2.7	1.2	3.9	2.3/1.0
	2.0	2.9	1.7	4.6	1.7/1.0
	4.0	2.5	1.3	3.8	1.9/1.0
	8.0	2.3	1.3	3.6	1.8/1.0
BTBPC + HCl (2.0 N)	1.0	2.3	1.2	3.5	1.9/1.0
	2.0	2.1	1.0	3.1	2.1/1.0
	4.0	3.1	2.0	5.1	1.6/1.0
	8.0	3.2	1.8	5.0	1.8/1.0
BTBPC + HCl (4.0 N)	1.0	2.5	1.4	3.9	1.8/1.0
	2.0	2.6	1.2	3.8	2.2/1.0
	4.0	3.9	2.1	6.0	1.9/1.0
	8.0	2.5	1.5	4.0	1.7/1.0
BTBPC + HCl (8.0 N)	1.0	1.7	1.4	3.1	1.2/1.0
	2.0	2.5	1.7	4.2	1.5/1.0
	4.0	2.5	1.6	4.1	1.6/1.0
	8.0	3.7	2.3	6.0	1.6/1.0

–: Not applicable

**Fig. 2** Thermal curves of heat flow versus temperature on BTBPC by DSC at heating rates of 1.0, 2.0, 4.0, and 8.0 $^\circ\text{C min}^{-1}$

release (ΔH_{max}), heat release of peak (ΔH_p), and total heat release (ΔH_t).

Figure 4 shows the results of heat production rate versus sample temperature of BTBPC alone and mixed with 1.0 or 2.0 N HCl. The thermal waveforms are very similar and almost have the same T_o and T_p value (Table 3).

BTBPC alone reveals just one single smooth exothermic peak and ca. 80.0 $^\circ\text{C}$ peak width spacing. From Table 3, T_o , T_p , ΔH_{max} , and ΔH_t were 125.3, 147.8 $^\circ\text{C}$, and 159.2 $\text{kJ kg}^{-1} \text{min}^{-1}$, 1032.0 kJ kg^{-1} , respectively. The right-side thermal waveforms of BTBPC with 1.0 and 2.0 N HCl mixtures are different from BTBPC alone. However, BTBPC with 1.0 or 2.0 N HCl mixtures is extremely similar to each other. Note that both 1.0 and 2.0 N HCl mixtures have a less obvious second exothermic peak at 175.6 and at 171.4 $^\circ\text{C}$, respectively. This peak does not appear in the BTBPC alone. The ΔH_t of BTBPC with 1.0 or 2.0 N mixture (1381.7 and 1237.2 kJ kg^{-1}) is higher than BTBPC alone (1032.0 kJ kg^{-1}), as listed in Table 3. It seems that the extra heat of reaction comes from part of the second exothermic reaction, which is induced by adding HCl. Figure 4 illustrates that the main reaction of BTBPC alone or mixed with 1.0, or 2.0 N HCl did not change. Nevertheless, BTBPC seems to be induced by 1.0 or 2.0 N HCl to produce second additional exothermic reactions. Reaction tends to be more complicated. This implies that the main reaction products combined with protons to induce further reactions and then prolonged the second exothermic response time.

Figure 5 shows the results of heat production rate versus sample temperature of BTBPC alone and high concentrated HCl mixtures, including 4.0 and 8.0 N HCl. Obviously,

Table 2 Peak data of the original thermal waveforms on BTBPC alone and mixed with various concentrations of HCl at different heating rates by DSC

Sample item	$\beta/^\circ\text{C min}^{-1}$	$T_o/^\circ\text{C}$	$T_p/^\circ\text{C}/\Delta H_{\text{max}}/\text{W g}^{-1}$		
			Peak A-1	Peak A	Peak A-2
BTBPC	1.0	111.5	–	130.8/0.8	–
	2.0	115.9	–	138.2/1.6	–
	4.0	125.3	–	148.0/2.6	–
	8.0	132.7	–	156.9/4.9	–
BTBPC + HCl (1.0 N)	1.0	104.1	–	130.7/1.1	–
	2.0	107.1	–	138.3/1.9	–
	4.0	123.0	–	148.0/3.0	–
	8.0	131.1	–	154.7/5.3	–
BTBPC + HCl (2.0 N)	1.0	102.1	103.0/1.2	131.5/0.6	169.3/0.2
	2.0	109.8	112.6/1.5	141.9/1.1	172.9/0.2
	4.0	123.5	–	147.8/2.9	–
	8.0	122.8	125.5/6.4	161.6/2.2	192.0/0.4
BTBPC + HCl (4.0 N)	1.0	71.0	85.9/1.0	–	154.7/0.2
	2.0	83.4	91.0/1.6	–	150.3/0.1
	4.0	89.2	101.6/2.9	–	177.4/0.3
	8.0	94.8	108.1/6.0	–	177.3/0.1
BTBPC + HCl (8.0 N)	1.0	40.2	67.6/0.9	–	130.1/0.3
	2.0	30.6	82.8/1.3	–	148.3/0.4
	4.0	46.1	79.6/2.2	–	175.0/0.7
	8.0	76.8	89.9/3.9	–	184.0/0.5

–: Not applicable

they reveal three completely different waveforms. Particularly, 4.0 N HCl mixture even starts with an exothermic reaction. Generally, 4.0 and 8.0 N HCl mixtures have two completely separated exothermic peaks. T_o (89.2 and 46.1 °C) and T_p (83.0 and 80.0 °C) occurred earlier than BTBPC alone ($T_o = 123.5$ and $T_p = 147.8$ °C), which means they will increase the risk of fire and explosion. Particularly, for the waveform of BTBPC with 4.0 N mixture, an obvious endothermic peak and two exothermic peaks appeared. First, a mild but significant endothermic peak ($\Delta H_{\text{max}} = 17.4 \text{ kJ kg}^{-1} \text{ min}^{-1}$) at ca. 70.0–83.0 °C appeared. A very violent exothermic reaction ($T_o = 89.2$ °C, $T_p = 101.2$ °C, and $\Delta H_{\text{max}} = 171.6 \text{ kJ kg}^{-1} \text{ min}^{-1}$) occurred at once. This doublet peak was split into a second peak at ca. 118.0 °C and increased the complexity of the decomposition reaction. Finally, the third relatively gentle exothermic reaction ($T_p = 176.8$ °C and $\Delta H_{\text{max}} = 15.6 \text{ kJ kg}^{-1} \text{ min}^{-1}$) arose slowly. It indicates that this decomposition reaction becomes more complex.

The waveform of BTBPC with 8.0 N HCl mixture appears with two exothermic peaks obviously, and there is not any significant endothermic peak. The first peaks of T_o (46.1 °C) and T_p (80.6 °C) are shifted down to lower temperature than 4.0 N mixture. In this exothermic peak, 8.0 N HCl mixture has a smaller ΔH_{max} ($125.0 \text{ kJ kg}^{-1} \text{ min}^{-1}$)

than all the other HCl mixtures, even if BTBPC alone. However, because this peak has the lowest T_o (46.1 °C), two split peaks, and large amount of total heat release (ΔH_t), we may reasonably conclude that this exothermic reaction is more complex and dangerous.

The T_p of the second exothermic peak of BTBPC with 4.0 and 8.0 N HCl mixtures (176.8 and 174.2 °C) is similar to BTBPC with 1.0 and 2.0 N HCl mixture (175.6 and 171.4 °C). Because of the bimodal separation, the second exothermic peaks of 4.0 and 8.0 N mixtures are clearly visible. As 4.0 N HCl mixture, ΔH_p of the first and the second exothermic waveforms are 904.2 and 113.4 kJ kg^{-1} , respectively. Similarly, as waveform of 8.0 N HCl mixture, the ΔH_p of the first exothermic peak is 877.3 kJ kg^{-1} . This value is likewise with the first exothermic peak of 4.0 N HCl mixture; however, the ΔH_p of the second exothermic peak in 8 N HCl mixture is 506.0 kJ kg^{-1} , which is ca. 4.5 times of 4.0 N HCl mixture. The total heat release (ΔH_t) of 8.0 N HCl mixture (1383.3 kJ kg^{-1}) is more than 4.0 N HCl mixture (991.6 kJ kg^{-1}) ca. 40.0 %. It reveals the decomposition reaction of 8.0 N HCl mixture is different from 4.0 N HCl mixture and seems more complicated and dangerous. Surprisingly all the BTBPC HCl mixtures have higher ΔH_t than BTBPC alone, except BTBPC with 4.0 N HCl

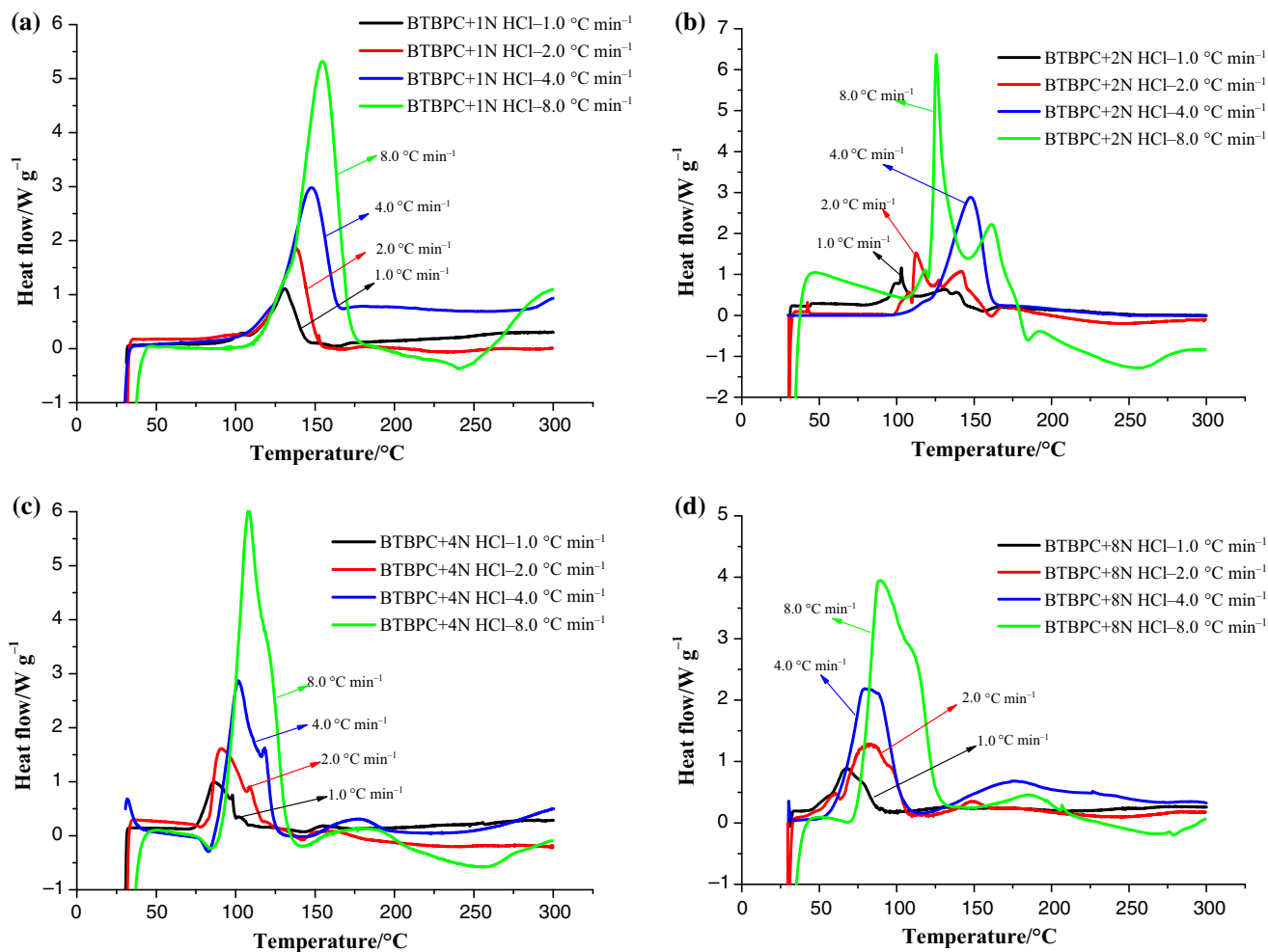


Fig. 3 Thermal curves of heat flow versus temperature on BTBPC mixed with 1.0, 2.0, 4.0, and 8.0 N HCl by DSC at heating rates of 1.0, 2.0, 4.0, and 8.0 °C min⁻¹

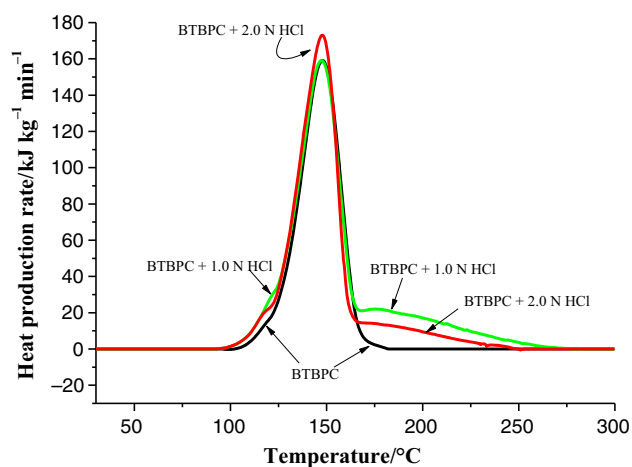


Fig. 4 Thermal waveforms of heat production rate versus temperature on BTBPC alone, 1.0 and 2.0 N HCl mixtures by DSC at 4.0 °C min⁻¹

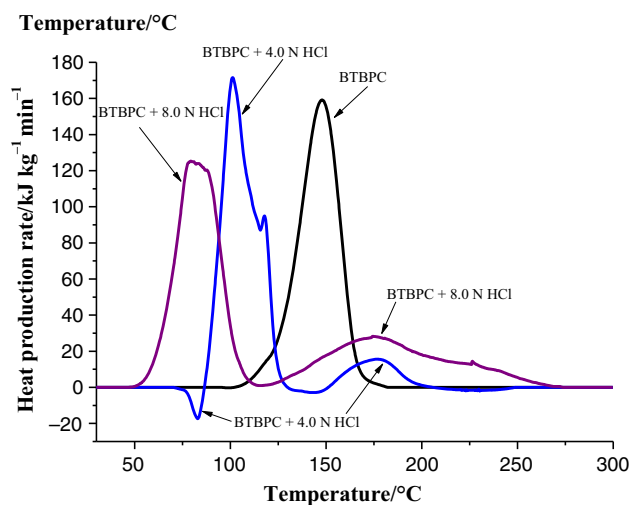


Fig. 5 Thermal waveforms of heat production rate versus temperature on BTBPC alone, 4.0 and 8.0 N HCl mixtures by DSC at 4.0 °C min⁻¹

Fig. 6 Thermal waveforms of thermic heat flow versus temperature on BTBPC alone and mixed with various normalities of HCl by DSC at 4.0 °C min⁻¹

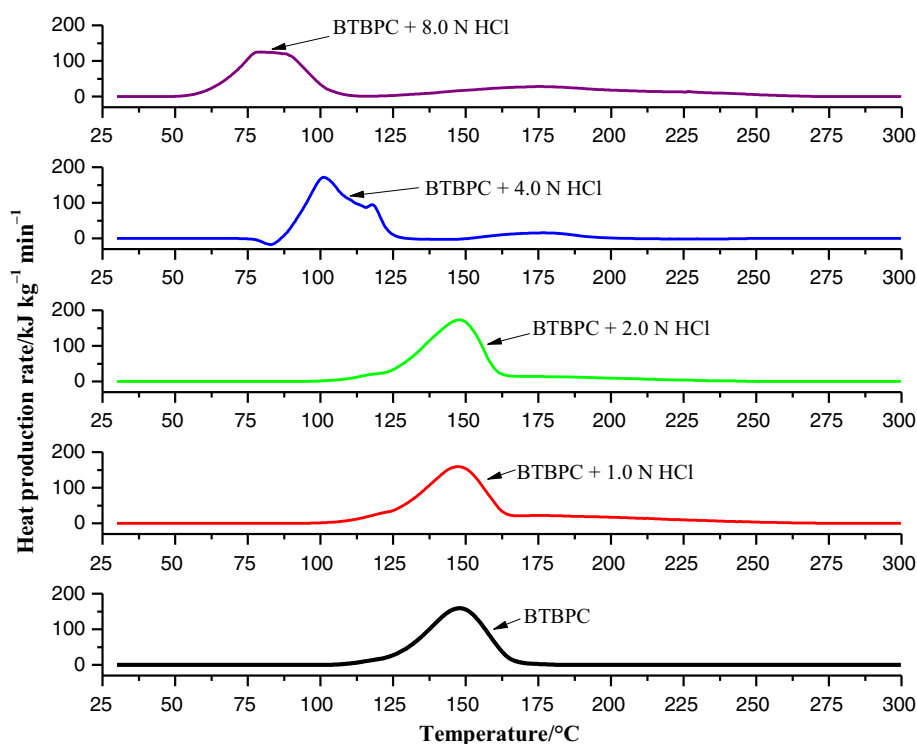


Table 3 Thermal stability kinetic parameters derived by STAR[®] from the DSC data sets on BTBPC and mixed with various concentrations of HCl at 4.0 °C min⁻¹

Sample item	Peak no.	$T_o/^\circ\text{C}$	$T_p/^\circ\text{C}$	$\Delta H_{\max}/\text{kJ kg}^{-1}\text{min}^{-1}$	$\Delta H_p/\text{kJ kg}^{-1}$	$\Delta H_t/\text{kJ kg}^{-1}$
BTBPC	1st	125.3	147.8	159.2	1032.0	1032.0
BTBPC + HCl (1.0 N)	1st	123.0	147.3	159.1	1082.0	–
	2nd	–	175.6	22.0	299.7	1381.7
BTBPC + HCl (2.0 N)	1st	123.5	147.8	173.1	1085.2	–
	2nd	–	171.4	14.3	289.0	1237.2
BTBPC + HCl (4.0 N)	1st	–	83.0	17.4	–26.0	–
	2nd	89.2	101.2	171.6	904.2	–
	3rd	–	176.8	15.6	113.4	991.6
BTBPC + HCl (8.0 N)	1st	46.1	80.6	125.0	877.3	–
	2nd	–	174.2	28.2	506.0	1383.3

mixture. The possible reason may be due to the influence of its first unusual endothermic reaction.

In Fig. 6, we collected all the waveforms of BTBPC alone and mixtures of different concentrations, here 1.0, 2.0, 4.0, and 8.0 N of HCl, to compare. They all have two exothermic peaks, but BTBPC alone has just only one exothermic peak. The first exothermic peak is significantly shifted to lower temperatures with increasing the levels of concentration of HCl. However, the second exothermic peak does not reveal a significant change, and T_p of the second exothermic peak is roughly ca. 171.0–177.0 °C. This case implies that the second exothermic peak was

induced by HCl, as an adulterant, but it is independent of HCl concentration.

Estimation of chemical kinetic model

Formal reaction stages

From the viewpoint of reaction kinetics, one reaction may include a step-by-step sequence of elementary reactions, which we called “reaction kinetic models.” However, restricted by the sensitivity of the measuring instrument, we could only directly observe the net chemical heat

change for most thermal reactions. In this study, we utilized the TSS simulation software to estimate the possible sequence of steps in reaction kinetic models.

Formal reaction stages are based upon the assumption that the conversion degrees are the state variables of a reacting system. Typically, we need to use such an approach when there is inadequate information for building up a more detailed reaction kinetic model, and only some overall responses are available from experiment, instead of the composition variation. Formal reaction stages can represent complex multistage reactions that may include several independent and consecutive stages [18]. The reaction stages are demonstrated in reaction Eqs. (1)–(20), and the following are what we found.

To clearly compare BTBPC alone and its contaminant mixtures of 1.0, 2.0, 4.0, and 8.0 N HCl, Figs. 7–11 demonstrate the thermal curves and their possible reaction kinetic models, respectively. The relevant thermokinetic parameters, such as formal reaction stage, kinetic model, reaction type, $\ln k_0$, E_a , n , z , ΔH_d , and k , are all presented in Table 4.

BTBPC alone

Figure 7 illustrates the results of heat production rate versus sample temperature of BTBPC alone. It reveals just one single smooth thermal peak. We used TSS simulation software to fit the thermal curve and tried to construct the possible model of reaction. It indicates that the decomposition reaction of BTBPC alone is a simple single-stage, n -order reaction. The reactant (0A) directly reacts with the products (0B). Equation (1) is the equation of the reaction rate for the reactant in the stage of reaction (r_{rtn}).

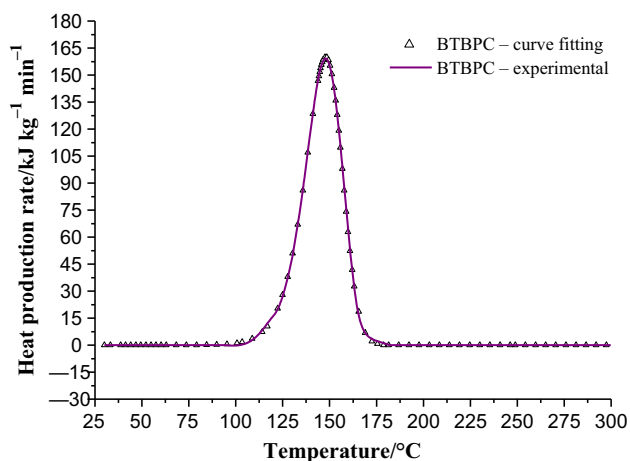


Fig. 7 Thermal curves of heat production rate versus temperature with kinetics-based curve fitting on BTBPC alone by DSC at $4.0\text{ }^\circ\text{C min}^{-1}$

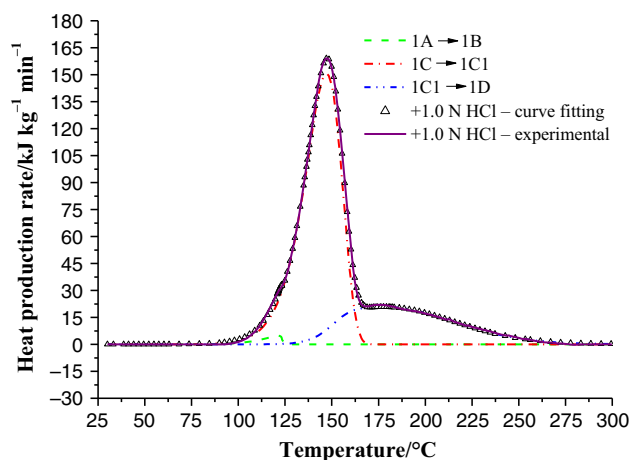


Fig. 8 Thermal curves of heat production rate versus temperature with kinetics-based curve fitting on BTBPC mixed with 1.0 N HCl by DSC at $4.0\text{ }^\circ\text{C min}^{-1}$

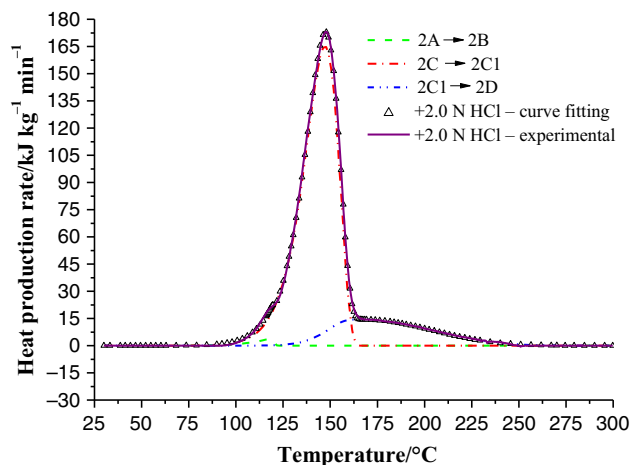


Fig. 9 Thermal curves of heat production rate versus temperature with kinetics-based curve fitting on BTBPC mixed with 2.0 N HCl by DSC at $4.0\text{ }^\circ\text{C min}^{-1}$

1. Simple single-stage reaction: $0A \rightarrow 0B$

$0A \rightarrow 0B$ n -order reaction

$$r_{0A} = \frac{d\alpha_{0A}}{dt} = k_0 e^{-\frac{E_a}{RT}} (1 - \alpha_{0A})^n \quad (1)$$

where α_{0A} is the degree of conversion for reactant 0A in the stage of reaction, from 0 to 1; k_0 and E_a denote the pre-exponential factor and apparent activation energy of this stage reaction. R is the ideal gas constant ($R = 8.314\text{ J mol}^{-1}\text{ K}^{-1}$), and n is the order of reaction. The relevant thermodynamic parameters, such as kinetic model, reaction type, reaction rate (r), natural logarithm of pre-exponential factor ($\ln k_0$), apparent activation energy (E_a),

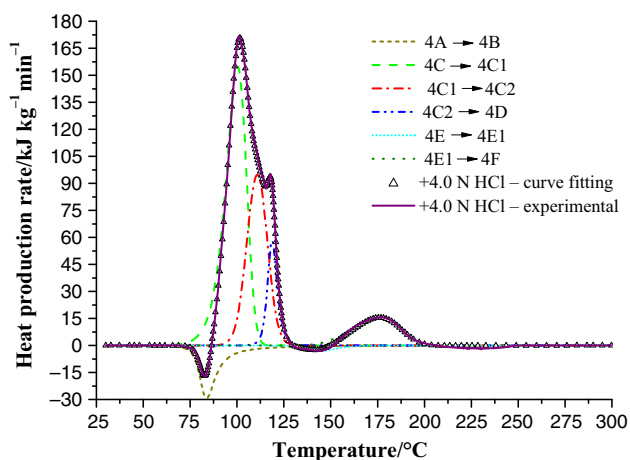


Fig. 10 Heat production rate versus temperature with kinetics-based curve fitting on BTBPC mixed with 4.0 N HCl by DSC at $4.0\text{ }^{\circ}\text{C min}^{-1}$

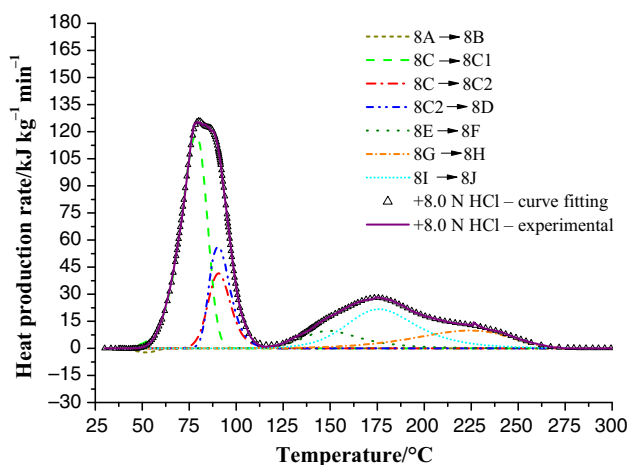


Fig. 11 Heat production rate versus temperature with kinetics-based curve fitting on BTBPC mixed with 8.0 N HCl by DSC at $4.0\text{ }^{\circ}\text{C min}^{-1}$

reaction order (n), heat of decomposition (ΔH_d), and rate constant (k), are given in Table 4.

BTBPC mixed with 1.0 and 2.0 N HCl

Figure 8 also demonstrates the results of heat production rate versus sample temperature of BTBPC with 1.0 N HCl mixture. The exothermic curves of BTBPC 1.0 N HCl mixture and BTBPC alone are different. There are two more slightly exothermic peaks on both sides of the main peak. One is on the left side ($113.0\text{ }^{\circ}\text{C}$) and the other is on the right side ($170.0\text{ }^{\circ}\text{C}$). In the same way, we applied TSS simulation software to fit this thermal curve. It indicates that the formal reaction is composed of a two-stage decomposition reaction. The first is an n -order simple

single-stage reaction ($1A \rightarrow 1B$); the second is two-consecutive-stage reaction ($1C \rightarrow 1C1 \rightarrow 1D$). Their equations of reaction rate for the reactant in each stage of reaction (r_{rcm}) are expressed by Eqs. (2)–(4).

1. Simple single-stage reaction: $1A \rightarrow 1B$

$1A \rightarrow 1B$ n -order reaction

$$r_{1A} = \frac{d\alpha_{1A}}{dt} = k_0 e^{-\frac{E_a}{RT}} (1 - \alpha_{1A})^n \quad (2)$$

2. Two-consecutive-stage reaction: $1C \rightarrow 1C1 \rightarrow 1D$

$1C \rightarrow 1C1$ n -order reaction

$$r_{1C} = \frac{d\alpha_{1C}}{dt} = k_0 e^{-\frac{E_a}{RT}} (1 - \alpha_{1C})^{n_1} \quad (3)$$

$1C1 \rightarrow 1D$ n -order reaction

$$r_{1C1} = \frac{d\alpha_{1C1}}{dt} = k_0 e^{-\frac{E_a}{RT}} (\alpha_{1C} - \alpha_{1C1})^{n_2} \quad (4)$$

where α_{1A} is the degree of conversion from the reactant 1A to product 1B; α_{1C} and α_{1C1} are the degree of conversion from the reactant 1C to intermediate product 1C1, and 1C1 to final product 1D, respectively; k_0 and E_a are the pre-exponential factor and apparent activation energy for each stage of reaction.

Both BTBPC with 1.0 and 2.0 N HCl mixtures have similar exothermic curves, as shown in Fig. 9. They also have two more slightly exothermic peaks on the both sides of the main peak: one on the left side ($113.0\text{ }^{\circ}\text{C}$) and the other on the right side ($170.0\text{ }^{\circ}\text{C}$). Fitting this thermal curve by TSS simulation software also reveals the formal reaction is composed of a two-stage decomposition reaction. The first is an n -order simple single-stage reaction ($2A \rightarrow 2B$), and the second is two-consecutive-stage reaction ($2C \rightarrow 2C1 \rightarrow 2D$). Their reaction rate (r_{rcm}) equations are expressed by Eqs. (5)–(7).

1. Simple single-stage reaction: $2A \rightarrow 2B$

$2A \rightarrow 2B$ n -order reaction

$$r_{2A} = \frac{d\alpha_{2A}}{dt} = k_0 e^{-\frac{E_a}{RT}} (1 - \alpha_{2A})^n \quad (5)$$

2. Two-consecutive-stage reaction: $2C \rightarrow 2C1 \rightarrow 2D$

$2C \rightarrow 2C1$ n -order reaction

$$r_{2C} = \frac{d\alpha_{2C}}{dt} = k_0 e^{-\frac{E_a}{RT}} (1 - \alpha_{2C})^{n_1} \quad (6)$$

$2C1 \rightarrow 2D$ n -order reaction

$$r_{2C1} = \frac{d\alpha_{2C1}}{dt} = k_0 e^{-\frac{E_a}{RT}} (\alpha_{2C} - \alpha_{2C1})^{n_2} \quad (7)$$

where α_{2A} is the degree of conversion from the reactant 2A to product 2B; α_{2C} and α_{2C1} are the degree of conversion from the reactant 2C to intermediate product 2C1, and 2C1 to final product 2D, respectively. The relevant

Table 4 Thermal stability kinetic parameters derived from TSS simulation data sets on BTBPC and mixed with various concentrations of HCl at 4.0 °C min⁻¹

Sample item	Formal reaction stage	Kinetic model	Reaction type	<i>r</i>	ln <i>k</i> ₀ /lns ⁻¹	<i>E</i> _a /kJ mol ⁻¹	<i>n</i>	<i>n</i> ₁	<i>n</i> ₂	<i>z</i>	Δ <i>H</i> _d /kJ kg ⁻¹	<i>k</i>
BTBPC	0A → 0B	0A → 0B	<i>n</i> order	<i>r</i> _{0A}	42.20	164.96	1.21	–	–	–	1030.73	8.58E–12
BTBPC + HCl (1.0 N)	1A → 1B	1A → 1B	<i>n</i> order	<i>r</i> _{1A}	32.93	124.43	0.19	–	–	–	17.55	1.35E–08
	1C → 1D	1C → 1C1	<i>n</i> order	<i>r</i> _{1C}	36.82	146.15	–	0.98	–	–	974.58	8.84E–11
BTBPC + HCl (2.0 N)	2A → 2B	1C1 → 1D	<i>n</i> order	<i>r</i> _{1C1}	5.32	44.14	–	–	1.24	–	395.18	2.80E–06
		2A → 2B	<i>n</i> order	<i>r</i> _{2A}	32.19	121.09	0.13	–	–	–	12.41	2.54E–08
	2C → 2D	2C → 2C1	<i>n</i> order	<i>r</i> _{2C}	37.87	149.78	–	0.88	–	–	990.24	5.74E–11
BTBPC + HCl (4.0 N)	4A → 4B	2C1 → 2D	<i>n</i> order	<i>r</i> _{2C1}	3.51	36.54	–	–	1.03	–	236.06	1.04E–05
		4A → 4B	Autocatalytic	<i>r</i> _{4A}	6.61	28.05	–	3.00	1.29	0.0002	–115.74	7.45E–03
	4C → 4D	4C → 4C1	<i>n</i> order	<i>r</i> _{4C}	66.58	220.57	–	1.12	–	–	553.06	4.09E–11
		4C1 → 4C2	<i>n</i> order	<i>r</i> _{4C1}	65.73	224.11	–	–	1.29	–	327.72	4.09E–12
	4E → 4F	4C2 → 4D	Autocatalytic	<i>r</i> _{4C2}	27.32	98.97	–	1.29	0.86	0.0122	101.34	1.71E–06
		4E → 4E1	<i>n</i> order	<i>r</i> _{4E}	71.56	264.22	–	2.05	–	–	–16.08	9.92E–17
BTBPC + HCl (8.0 N)	8A → 8B	4E1 → 4F	<i>n</i> order	<i>r</i> _{4E1}	28.98	127.88	–	–	1.04	–	122.27	6.24E–11
		8A → 8B	<i>n</i> order	<i>r</i> _{8A}	54.63	159.74	1.09	–	–	–	–8.48	1.82E–05
	8C → 8D	8C → 8C1	<i>n</i> order	<i>r</i> _{8C}	49.95	159.45	–	1.14	–	–	533.78	1.91E–07
		8C1 → 8C2	Autocatalytic	<i>r</i> _{8C1}	64.87	209.38	–	1.74	0.01	0.0180	160.92	7.29E–10
		8C2 → 8D	Autocatalytic	<i>r</i> _{8C2}	39.68	125.62	–	0.91	0.35	0.0138	199.92	7.05E–06
	8E → 8F	8E → 8F	<i>n</i> order	<i>r</i> _{8E}	45.46	176.83	2.99	–	–	–	101.72	1.71E–12
	8G → 8H	8G → 8H	<i>n</i> order	<i>r</i> _{8G}	12.55	76.70	0.93	–	–	–	159.16	6.05E–09
8I → 8J	8I → 8J	<i>n</i> order	<i>r</i> _{8I}	32.58	141.20	2.36	–	–	–	272.04	9.75E–12	

$$k = \exp(\ln k_0 - \frac{E_a \times 1000}{RT}), T = 293.15 \text{ K}$$

thermodynamic parameters and reaction type of BTBPC with 1.0 and 2.0 N HCl mixtures are all listed in Table 4. According to the heat of decomposition (Δ*H*_d), the second formal reaction (1C → 1D, 2C → 2D) is the major reaction, where the initial kinetic model (1C → 1C1, 2C → 2C1) is an intense reaction, and then the follow-up reaction (1C1 → 1D, 2C1 → 2D) is a relatively mild, but prolonged reaction. Otherwise, the first reaction (1A → 1B, 2A → 2B) is a minor and very weak reaction; however, it seems to occur simultaneously with the second reaction.

BTBPC mixed with 4.0 N HCl

The results of heat production rate versus sample temperature of BTBPC with 4.0 N HCl mixture are shown in Fig. 10. This thermal curve includes two main exothermic peaks and another two slight endothermic peaks. It is more complicated than BTBPC with other lower HCl (1.0 and 2.0 N) mixtures. The results of using TSS simulation software to fit this thermal curve demonstrate that the formal reaction is composed of a three-stage decomposition

reaction. First is an autocatalytic simple single-stage reaction (4A → 4B); furthermore, a three-consecutive-stage reaction appears (4C → 4C1 → 4C2 → 4D). Finally, a two-consecutive-stage reaction (4E → 4E1 → 4F) comes out to finish the reaction. Their reaction rate (*r*_{rcm}) equations are expressed by the following Eqs. (8)–(13), respectively.

- (1) Simple single-stage reaction: 4A → 4B

$$4A \rightarrow 4B \text{ autocatalytic reaction}$$

$$r_{4A} = \frac{d\alpha_{4A}}{dt} = k_0 e^{\frac{-E_a}{RT}} (1 - \alpha_{4A})^{n1} (\alpha_{4A}^{n2} + z) \tag{8}$$

- (2) Three-consecutive-stage reaction: 4C → 4C1 → 4C2 → 4D

$$4C \rightarrow 4C1 \text{ } n\text{-order reaction}$$

$$r_{4C} = \frac{d\alpha_{4C}}{dt} = k_0 e^{\frac{-E_a}{RT}} (1 - \alpha_{4C})^{n1} \tag{9}$$

$$4C1 \rightarrow 4C2 \text{ } n\text{-order reaction}$$

$$r_{4C1} = \frac{d\alpha_{4C1}}{dt} = k_0 e^{\frac{-E_a}{RT}} (\alpha_{4C} - \alpha_{4C1})^{n2} \tag{10}$$

4C2 → 4D autocatalytic reaction

$$r_{4C2} = \frac{d\alpha_{4C2}}{dt} = k_o e^{\frac{-E_a}{RT}} (\alpha_{4C1} - \alpha_{4C2})^{n_1} (\alpha_{4C2}^{n_2} + z) \quad (11)$$

3. Two-consecutive-stage reaction: 4E → 4E1 → 4F

4E → 4E1 *n*-order reaction

$$r_{4E} = \frac{d\alpha_{4E}}{dt} = k_o e^{\frac{-E_a}{RT}} (1 - \alpha_{4E})^{n_1} \quad (12)$$

4E1 → 4F *n*-order reaction

$$r_{4E1} = \frac{d\alpha_{4E1}}{dt} = k_o e^{\frac{-E_a}{RT}} (\alpha_{4E} - \alpha_{4E1})^{n_2} \quad (13)$$

The related thermodynamic parameters and reaction models of BTBPC with 4.0 N mixtures are all presented in Table 4. Based on the data of ΔH_d , the second formal reaction (4C → 4D) was fierce and accounted for a large heat proportion of total heat release. Thus, this formal reaction is the major reaction. Particularly, ΔH_d decreased with different stages of the reaction. For instance, the heat release of kinetic model 4C → 4C1, 4C1 → 4C2, and 4C2 → 4D is 553.1, 327.7, and 101.3 kJ kg⁻¹, respectively. Reaction 4A → 4B is an apparent small endothermic autocatalytic reaction, and 4C → 4C1 is a major exothermic *n*-order reaction of 4C → 4D. They almost occurred at the same time. Reaction 4E → 4F is a gentle exothermic reaction; its temperature interval is shorter than another concentration of HCl-mixed BTBPC.

BTBPC mixed with 8.0 N HCl

Figure 11 shows the results of heat production rate versus sample temperature of BTBPC with 8.0 N HCl mixture. There are two main exothermic peaks which show different thermal curve from BTBPC with other HCl (1.0, 2.0, and 4.0 N) mixture. Prior to the first exothermic peak, an endothermic peak emerges. However, the heat of absorption is very small and not obvious. The TSS fitting results indicated that the formal reaction is composed of a five-stage decomposition reaction. First is an *n*-order simple single-stage reactions (8A → 8B); the second is a three-consecutive-stage reaction (8C → 8C1 → 8C2 → 8D); and finally, three successive *n*-order simple single-stage reactions (8E → 8F, 8G → 8H, 8I → 8 J) occurred and finished the reaction. All the reaction rate (r_{rctn}) equations are expressed by the following Eqs. (14)–(20), respectively.

1. Simple single-stage reaction: 8A → 8B

8A → 8B *n*-order reaction

$$r_{8A} = \frac{d\alpha_{8A}}{dt} = k_o e^{\frac{-E_a}{RT}} (1 - \alpha_{8A})^n \quad (14)$$

2. Three-consecutive-stage reaction:

8C → 8C1 → 8C2 → 8D

8C → 8C1 *n*-order reaction

$$r_{8C} = \frac{d\alpha_{8C}}{dt} = k_o e^{\frac{-E_a}{RT}} (1 - \alpha_{8C})^{n_1} \quad (15)$$

8C1 → 8C2 autocatalytic reaction

$$r_{8C1} = \frac{d\alpha_{8C1}}{dt} = k_o e^{\frac{-E_a}{RT}} (\alpha_{8C} - \alpha_{8C1})^{n_1} (\alpha_{8C1}^{n_2} + z) \quad (16)$$

8C2 → 8D autocatalytic reaction

$$r_{8C2} = \frac{d\alpha_{8C2}}{dt} = k_o e^{\frac{-E_a}{RT}} (\alpha_{8C1} - \alpha_{8C2})^{n_1} (\alpha_{8C2}^{n_2} + z) \quad (17)$$

3. Simple single-stage reaction: 8E → 8F

8E → 8F *n*-order reaction

$$r_{8E} = \frac{d\alpha_{8E}}{dt} = k_o e^{\frac{-E_a}{RT}} (1 - \alpha_{8E})^n \quad (18)$$

4. Simple single-stage reaction: 8G → 8H

8G → 8H *n*-order reaction

$$r_{8G} = \frac{d\alpha_{8G}}{dt} = k_o e^{\frac{-E_a}{RT}} (1 - \alpha_{8G})^n \quad (19)$$

5. Simple single-stage reaction: 8I → 8 J

8I → 8J *n*-order reaction

$$r_{8I} = \frac{d\alpha_{8I}}{dt} = k_o e^{\frac{-E_a}{RT}} (1 - \alpha_{8I})^n \quad (20)$$

All the related thermokinetic parameters and reaction model of BTBPC with 8.0 N mixtures are listed in Table 4. The reaction occurs in advance to 50.0 °C. 8A → 8B is a minor endothermic *n*-order reaction, whereas 8C → 8C1 is a major exothermic *n*-order reaction. They almost occurred simultaneously. According to the data of ΔH_d , the second formal reaction (8C → 8D) is a major reaction. ΔH_d decreased irregularly with different stages of the kinetic model. The heat release of 8C → 8C1, 8C1 → 8C2, and 8C2 → 8D is 533.8, 160.9, and 199.9 kJ kg⁻¹, respectively. 8E → 8F, 8G → 8H, and 8I → 8 J are three successively appearing kinetic models. ΔH_d is increased with different reactions, which are 101.7, 159.2, and 272.0 kJ kg⁻¹, respectively.

The reaction curve 8G → 8H also appears in the curve of 1 N (1C1 → 1D), 2 N (2C1 → 2D), and 4 N (4E1 → 4F) HCl mixtures. However, 8E → 8F and 8I → 8 J do not appear in the curve of 1.0, 2.0, and 4.0 N HCl mixtures. They are new reactions, that is, the decomposition reaction of BTBPC mixed with 8.0 N HCl mixture illustrates more complexity than BTBPC mixed with the other lower normality (1.0, 2.0, and 4.0 N) of HCl mixtures.

Conclusions

This study adopted an improved TSS method on DSC for 70.0 mass% BTBPC alone and mixed with 1.0, 2.0, 4.0, and 8.0 N HCl to acquire thermal runaway data and thermokinetic parameters. Based on the experimental and simulated investigation at 4.0 °C min⁻¹ heating rate, the conclusions can be summarized as follows:

1. BTBPC alone and BTBPC mixed with 1.0 and 2.0 N HCl mixture all reveal one single smooth exothermal peak. 1.0 and 2.0 N HCl mixtures have a less obvious second exothermic peak at ca. 170.0 °C, and the total heat release of 1 and 2.0 N mixtures is higher than BTBPC alone.
2. T_o and T_p of BTBPC with 4.0 N HCl mixture are both shifted down to lower temperature (89.2, 101.2 °C) than BTBPC alone, 1.0, and 2.0 N mixtures. Particularly, 4.0 N HCl mixture has an endothermic peak and two exothermic peaks. The first exothermic peak is a very violent doublet peak which was split at ca. 118.0 °C. This decomposition reaction became more complicated, but with no change in total heat release.
3. For BTBPC with 8.0 N HCl mixture, two exothermic peaks appear, but no significant endothermic peak. The first peaks of T_o and T_p are shifted down to lower temperature (46.1, 80.6 °C) than 4.0 N mixture. The total heat release (ΔH_t) of 8.0 N HCl mixture (1383.3 kJ kg⁻¹) is more than 4.0 N HCl mixture (991.7 kJ kg⁻¹) at ca. 40.0 %. It indicates the decomposition reaction of BTBPC with 8.0 N HCl mixture is more complicated and dangerous.
4. All the BTBPC HCl mixtures have a second exothermic peak at ca. 170.0 °C. Peaks on 1.0 and 2.0 N HCl mixtures are less prominent, but on 4.0 and 8.0 N HCl mixture are fully separated and obvious. The first exothermic peak is prominently shifted to lower temperatures with increasing the levels of concentration of HCl, but T_p of the second exothermic peak did not reveal significant change. This implies that the second exothermic peak was induced by HCl being used; however, it is independent of HCl concentration. All the BTBPC HCl mixtures have more ΔH_t than BTBPC alone, but BTBPC with 4.0 N HCl mixture. We surmise that the possible reason is because of the influence of an unusual endothermic reaction. Moreover, the ΔH_t of the second exothermic peak on 8 N HCl mixture is ca. 4.5-fold of 4.0 N HCl mixture.
5. BTBPC alone is a simple n -order single-stage reaction. After BTBPC is mixed with HCl, the kinetic models of decomposition reaction become more complex. BTBPC mixed with either 1.0 or 2.0 N HCl is composed of a two-stage decomposition reaction.

Moreover, 4.0 or 8.0 N HCl mixture is three- and five-stage decomposition reactions, respectively.

6. The initial reactions of BTBPC with 4.0 and 8.0 N HCl mixture are endothermic reactions. 4.0 N HCl mixture is an apparently small endothermic autocatalytic reaction, and the 8.0 N HCl mixture is a not obviously a minor endothermic n -order reaction. They were both accompanied by a three-consecutive-stage major exothermic reaction.

Acknowledgements The authors wish to express their gratitude to Dr. Arcady A. Kossov of ChemInform Saint Petersburg (CISP), Ltd., St. Petersburg, Russia, for providing technical assistance. The authors would also like to thank Ms. Min-Siou Liao for her help on the measurements of runaway tests.

References

1. Bach RD, Ayala PY, Schlegel HB. A reassessment of the bond dissociation energies of peroxides. An ab initio study. *J Am Chem Soc.* 1996;118:12758–65.
2. Bretherick L. In: Young JA, editor. Improving safety in the chemical laboratory: a practical guide. Wiley: New York; 1987.
3. Chang YM, You ML, Lin CH, Wu SY, Tseng JM, Lin CP, Wang YL, Shu CM. Fire and explosion hazard evaluation for the acetone aqueous solutions. *J Therm Anal Calorim.* 2011;106:179–89.
4. Tsai LC, You ML, Ding MF, Shu CM. Thermal hazard evaluation of lauroyl peroxide mixed with nitric acid. *Molecules.* 2012;17:8056–67.
5. March J. Advanced organic chemistry: reactions, mechanisms, and structure. 5th ed. New York: Wiley; 1992.
6. Wang TS, Liu SH, Qian XM, Shu CM. Isothermal hazards evaluation of benzoyl peroxide mixed with benzoic acid via TAM III test. *J Therm Anal Calorim.* 2013;113:1625–31.
7. Chi JH, Wu SH, Charpentier JC, Yet-Pole I, Shu CM. Thermal hazard accident investigation of hydrogen peroxide mixing with propanone employing calorimetric approaches. *J Loss Prevent Proc.* 2012;25:142–7.
8. Liu SH, Hou HY, Shu CM. Effects of thermal runaway hazard for three organic peroxides conducted by acids and alkalines with DSC, VSP2, and TAM III. *Thermochim Acta.* 2013;566:226–32.
9. Li AC, Tsai YT, Wu SH, Chiu CW, Shen SJ, Chang RH, Shu CM. Thermal runaway analyses for two organic peroxides with H₂O and dry fire-extinguishing chemicals by DSC and VSP2. *J Therm Anal Calorim.* 2013;113:1611–8.
10. Hsueh KH, Chen WT, Chu YC, Tsai LC, Shu CM. Thermal reactive hazards of 1,1-bis(*tert*-butylperoxy)cyclohexane with nitric acid contaminants by DSC. *J Therm Anal Calorim.* 2012;109:1253–60.
11. Villalobos MA, Hamielec AE, Wood PE. Kinetic model for short-cycle bulk styrene polymerization through bifunctional initiators. *J Appl Polym Sci.* 1991;42:629–37.
12. Drumright RE, Kastl PE, Priddy DB. Cycloalkane perketal initiators for styrene polymerization. 1. Decomposition chemistry of 1, 1-bis(*tert*-butylperoxy)cyclohexane. *Macromolecules.* 1993; 26:2246–52.
13. High Pressure Crucible, Non-Reusable (DSC), Mettler-Toledo International Inc., 2014. From http://ca.mt.com/ca/en/home/products/Laboratory_Analytics_Browse/TA_Family_Browse/ta_sumable_browse/00026731_1.html.

14. STAR[®] Thermal Analysis Software with Solaris Operating System, Operating Instructions, Mettler-Toledo International Inc. 2014. From http://us.mt.com/us/en/home/products/Laboratory_Analytics_Browse/TA_Family_Browse/TA_software_browse.html.
15. Hou HY, Shu CM, Duh YS. Exothermic decomposition of cumene hydroperoxide at low temperature conditions. *AIChE J.* 2001;47(8):1893–6.
16. Kossoy AA, Koludarova E. Specific features of kinetics evaluation in calorimetric studies of runaway reactions. *J Loss Prevent Proc.* 1995;8(4):229–35.
17. Kossoy A, Akhmetshin Y. Identification of kinetic models for the assessment of reaction hazards. *Process Saf Prog.* 2007; 26:209–20.
18. Chen JR, Cheng SY, Yuan MH, Kossoy A, Shu CM. Hierarchical kinetic simulation for autocatalytic decomposition of cumene hydroperoxide at low temperatures. *J Therm Anal Calorim.* 2009;96:751–8.
19. Talouba B, Balland L, Mouhab N, Abdelghani-Idrissi MA. Kinetic parameter estimation for decomposition of organic peroxides by means of DSC measurements. *J Loss Prev Process Ind.* 2011;24:391–6.
20. Uchida T, Wakakura M, Miyake A, Ogawa T. Thermal decomposition of organic peroxide with metals using calorimeters. *J Therm Anal Calorim.* 2008;93:47–52.
21. Xinrui L, Koseki H, Iwata Y, Mok YS. Decomposition of methyl ethyl ketone peroxide and mixtures with sulfuric acid. *J Loss Prev Process Ind.* 2004;17(1):23–8.